Supplement of Atmos. Chem. Phys., 26, 11047–11066, 2026
https://doi.org/10.5194/acp-26-11047-2026-supplement

Atmospheric Chemistry and Physics
Open Access
EGU

Supplement of

Characterizing emissions, chemistry, and health impacts of aged wildfire smoke in a western US city

Lixu Jin et al.

Correspondence to: Lixu Jin (lixu.jin@umontana.edu)

S1 Enhancement ratio and photochemical age

BB enhancement ratios (EnRs). An EnR for a species X is defined as the ratio of its excess mixing ratio ΔX to that of carbon monoxide (CO) during BB-impacted periods ($EnR_X(t) = \frac{\Delta X(t)}{\Delta CO(t)}$), where $\Delta X(t) = X_{obs}(t) - X_{bkg}(t)$. Compound-specific backgrounds X_{bkg} were derived separately for weekdays and weekends from HMS-identified no-fire days representative of local urban conditions.

We report two EnR types: (i) dynamic EnR at hourly resolution ($EnR_X(h) = \frac{\Delta X(h)}{\Delta CO\ (h)}$) and (ii) event-integrated EnR for each smoke window ($EnR_X = \frac{\sum \Delta X}{\sum \Delta CO}$). Because dynamic EnRs are sensitive to urban background selection, in addition to using the median values, we also use the 25th and 75th percentiles of the no-fire data to derive the weekday-weekend diurnal profiles for urban background profiles as sensitivity tests. The sensitivity tests change the EnRs within 20%, but do not change the overall conclusions of this work. We treat this ±20% range as the dominant EnR uncertainty associated with background selection.

Photochemical age. Plume photochemical age is estimated using the toluene-to-benzene clock (de Gouw et al., 2017). Assuming co-emission and first-order OH loss, OH exposure is derived as follows:

$$\int_0^t [OH]dt = \frac{1}{(k_{TOL} - k_{BENZ})} \times \left(\ln\left(\frac{[TOL]}{[BENZ]}|_{t(0)}\right) - \ln\left(\frac{[TOL]}{[BENZ]}|_{t(i)}\right)\right) \quad \text{Eq. (S1)}$$

where $\int_0^t [OH]dt$ is OH exposure, and k_{TOL} and k_{BENZ} are gas-phase OH rate constants for toluene and benzene (k_{TOL} = 5.63 × 10^{-12} and k_{BENZ} = 1.22 × 10^{-12} cm³ molecule⁻¹ s⁻¹). The emission ratio $\left(\frac{[TOL]}{[BENZ]}|_{t(0)}\right)$ is taken from the WE-CAN aircraft campaign for western US wildfires (0.7 ppbv/ppbv) (Permar et al., 2021). $\frac{[TOL]}{[BENZ]}|_{t(i)}$ is the dynamic enhancement ratio of toluene relative to benzene, and is calculated from the hourly measurements. We report the photochemical age by dividing the calculated OH exposure by the assumed average daytime OH concentration (1 × 10^6 molecules cm^{-3}) (Koss et al., 2018; Permar et al., 2021).

Link to emission ratios and OH rate constants.

Using the relationship between EnRs and photochemical age, we retrieve emission ratios (ERs) for primary VOCs and the gas-phase OH loss rate constant (k_{X+OH}). For a species X whose loss is dominated by a first-order reaction with OH radicals (e.g., hydrocarbons), the temporal evolution of its enhancement can be described as:

$$\frac{d\Delta X}{dt} = -k_{X+OH}[OH]\Delta X \quad \text{Eq. (S2)}$$

where $\Delta X = X_{obs} - X_{bkg}$. Here, X_{obs} and X_{bkg} are the observed and background mixing ratios of X, respectively. The term [OH] refers to an effective average concentration used to infer cumulative OH exposure, rather than directly measured real-time values.

Integrating Eq. (S2) gives

$$\Delta X(t) = \Delta X_0 \, e^{-k_{X+OH} \times \int_0^t [OH] dt} \qquad \text{Eq. (S3)}$$

where ΔX_0 is the initial enhancement.

Applying Eq. (S3) to both X and CO, and defining the enhancement ratio of species X relative to CO as

$$EnR_X(t) = \frac{\Delta X\ (t)}{\Delta CO\ (t)}$$

yields

$$EnR_X(t) = ER_X \times e^{-(k_{X+OH} - k_{CO+OH}) \times \int_0^t [OH] dt} \qquad \text{Eq. (S4)}$$

where

$$ER_X = \frac{\Delta X\ (0)}{\Delta CO\ (0)}$$

is the emission ratio of X relative to CO at the source.

Taking natural logarithms of Eq. (S4) yields a linearized form suitable for regression analysis:

$$\ln EnR_X(t) = -(k_{X+OH} - k_{CO+OH}) \times [OH]_{avg} \times t + \ln ER_X \qquad \text{Eq. (S5)}$$

where $[OH]_{avg}$ is the assumed mean OH concentration (1×10^6 molecules cm^{-3}) used to convert time to effective OH exposure.

When regressing $\ln EnR_X(t)$ against time t, the intercept b corresponds to the extrapolated emission ratio

$$ER_X = e^b \qquad \text{Eq. (S6)}$$

while the slope m reflects the differential OH reactivity between X and CO:

$$k_{X+OH} = k_{CO+OH} - \frac{m}{[OH]_{avg}} \qquad \text{Eq. (S7)}$$

For oxygenated VOCs that are substantially produced within the plume (e.g., acetone or acetaldehyde), the $\ln EnR_X$–time relationship often deviates from linearity due to concurrent

production and loss. In these cases, the intercept no longer represents a true emission ratio, and the slope should be interpreted qualitatively as indicating net production (positive) or net loss (negative) rather than as a quantitative OH rate constant. Thus, we focus our analysis on primary VOCs here.

Uncertainty analysis. The ER/EnR retrieval is most sensitive to three method choices: (1) Initial ratio used by the photochemical clock ($[TOL]/[BENZ]$ at $t = 0$). Using alternative initial ratios (field-based vs laboratory-based) shifts inferred OH exposure and retrieved time-zero ERs for benzene, toluene, and C8 aromatics by ~10–40% (Koss et al., 2018; Permar et al., 2021). (2) Background definition (X_{bkg}). Using the 25th–75th percentile no-fire profiles as alternative backgrounds changes EnRs by ~20%, which we treat as the dominant EnR uncertainty associated with background selection. (3) Use of benzene/toluene as a clock in aged, mixed smoke. Mixing and periods when toluene approaches background can increase clock noise and uncertainty in extrapolated ERs. We assess this uncertainty with a GEOS-Chem synthetic-truth test, in which GEOS-Chem is treated as an idealized case with known GFAS-based ERs, and the method is evaluated by comparing inferred ERs with the model's true ERs. This test shows ~10% agreement, suggesting the robustness of the photochemical clock estimate in the ideal, simplified model scenario, though in observations, larger uncertainties, as mentioned above, exist and are hard to resolve.

S2 Public health risk assessment

We assess both cancer and non-cancer inhalation risks following the U.S. EPA AirToxScreen framework (US EPA, 2022). These estimates represent upper bounds because we assume that the wildfire smoke conditions seen in September 2020 occur every year for a full 70-year lifetime.

Exposure metric. Hourly observations during smoke-impacted periods were averaged to obtain the mean "smoke-hour" concentration (C_{smoke}). For this study, C_{smoke} is defined as the average concentration across all smoke-impacted days in September 2020. To annualize exposure, we compute: $C_{annual} = f_{smoke} \times C_{smoke}$, where f_{smoke} is the local climatological smoke frequency, defined as the ratio of smoke-impacted hours to total hours in a year, based on 2010–2024 records (Fig. 1). A smoke-impacted hour is identified when the hourly $PM_{2.5}$ concentration exceeds 15 μg m^{-3} during wildfire season (June–October) and coincides with active smoke detected by the NOAA HMS smoke plume product. For Missoula, the 2010–2024 historical climatology indicates a mean 664 ± 445 smoke-impacted hours per year, corresponding to f_{smoke}= (664 ± 445) / 8,760 ≈ 0.08 ± 0.05, equivalent to approximately 29 ± 17 smoke-impacted days per year—roughly one month of smoke-impacted conditions annually**.**

Cancer risk (chronic). Incremental lifetime cancer risk (ILCR) for carcinogen i was

$$ILCR_i = URE_i \times C_{annual,i}$$

where URE_i (unit risk estimate; per μg m^{-3}) is the excess lifetime cancer risk associated with continuous inhalation of every 1 μg m^{-3} carcinogen i over a 70-year lifetime, assuming a linear no-threshold model. Combined cancer risk is reported as $ILCR_{total} = \sum_i ILCR_i$ and expressed as excess cases per million people due to wildfire smoke. For $PM_{2.5}$, for which no pollutant-specific

URE is available, we used the median URE for polycyclic aromatic hydrocarbons (PAHs) (4.8×10^{-5} per $\mu g \cdot m^{-3}$) as a proxy (Pye et al., 2024). URE values for seven measured HAPs were taken from EPA IRIS and OEHHA (OEHHA, 2025; US EPA, 2026). There is no established metric for "acute cancer risk." Short smoke episodes contribute only through their small, time-weighted addition to long-term exposure, which is already captured by the chronic ILCR calculation.

Non-cancer risk (chronic and acute). Non-cancer risks were expressed as hazard quotients (HQ) using three averaging times: annual, 1-h, and 8-h. For species i and averaging time τ,

$$HQ_{\tau,i} = \frac{C_{\tau,\mathrm{i}}}{RfC_{\tau,i}}$$

where τ represents one of the following averaging times: annual, 1 hour, or 8 hours. For chronic assessments, C_{annual} was taken as the annualized concentration defined in the "Exposure metric" section. For acute assessments, $C_{1h,i}$ and C8h,i were defined as the maximum 1-h average concentration and maximum 8-h moving-average concentration, respectively, observed during the September 2020 smoke period. Hazard indices (HI) were obtained by summing HQs across species affecting the same target organ/system; HI>1 indicates air toxics are likely to cause adverse health effects (US EPA, 2022). Chronic and acute HIs are reported separately and not combined.

For $PM_{2.5}$, we used the diesel-particulate reference concentration (RfC) of 5 μg m^{-3} for chronic risks (Pye et al., 2024). No acute RfC is available for $PM_{2.5}$; therefore, acute $PM_{2.5}$ risk is not evaluated. For HAPs, RfC values were derived from OEHHA, NIOSH and the EPA (CDC, 2020; OEHHA, 2023; US EPA, 2022). For reference, the UREs and RfCs used in this analysis are summarized in Table S1.

Table S1. Summary of inhalation toxicity reference values and sources for selected compounds.

Compound	URE	Reference (cancer)	1-hr REL	Reference (acute)	8-hr REL	Reference (8-hr)	Chronic RfC	Reference (chronic)
1,3-Butadiene	0.00017	OEHHA	660.0	OEHHA	9.0	OEHHA	2.0	OEHHA
Acetaldehyde	3e-06	OEHHA	470.0	OEHHA	300.0	OEHHA	9.0	EPA IRIS
Acetonitrile	N/A	N/A	N/A	N/A	34000.0	NIOSH	60.0	EPA IRIS
Acrolein	N/A	N/A	2.5	OEHHA	0.7	OEHHA	0.02	EPA IRIS
Acrylonitrile	0.00029	OEHHA	N/A	N/A	N/A	N/A	2.0	EPA IRIS
Benzene	2.9e-05	OEHHA	27.0	OEHHA	3.0	OEHHA	3.0	OEHHA
C8 aromatics	N/A	N/A	22000.0	OEHHA (C8 aromatics)	435000.0	NIOSH	100.0	EPA IRIS
C9 aromatics	N/A	N/A	2400.0	OEHHA (TMBs)	8.0	OEHHA (TMBs)	4.0	OEHHA

Compound	URE	Reference (cancer)	1-hr REL	Reference (acute)	8-hr REL	Reference (8-hr)	Chronic RfC	Reference (chronic)
Dichlorobenzene	1.1e-05	OEHHA (1,4-DCB)	8700.0	OEHHA (1,4-DCB)	5.0	OEHHA (1,4-DCB)	10.0	OEHHA
Formaldehyde	1.1e-05	EPA IRIS (2024)	55.0	OEHHA	9.0	OEHHA	7.0	EPA IRIS
Furfural	N/A	N/A	N/A	N/A	N/A	N/A	N/A	N/A
MEK	N/A	N/A	13000.0	OEHHA	N/A	N/A	N/A	N/A
Maleic anhydride	N/A	N/A	N/A	N/A	N/A	N/A	0.7	OEHHA
Methanol	N/A	N/A	28000.0	OEHHA	26000.0	NIOSH	4000.0	OEHHA
Methyl isocyanate	N/A	N/A	N/A	N/A	50.0	NIOSH	1.0	OEHHA
Methyl methacrylate	N/A	N/A	N/A	N/A	410000.0	NIOSH	700.0	EPA IRIS
Methyl styrenes	N/A	N/A	N/A	N/A	N/A	N/A	N/A	N/A
Methylglyoxal	N/A	N/A	6000.0	Proxy: Acrylic acid (OEHHA)	N/A	N/A	N/A	N/A
Naphthalene	3.4e-05	OEHHA	N/A	N/A	50000.0	NIOSH	9.0	OEHHA
Nitromethane	N/A	N/A	N/A	N/A	250000.0	NIOSH	N/A	N/A
PM2.5	4.8e-05	Pye et al., 2024	N/A	N/A	N/A	N/A	5.0	Pye et al., 2024
Phenol	N/A	N/A	5800.0	OEHHA	19000.0	NIOSH	200.0	OEHHA
Propanol	N/A	N/A	3200.0	OEHHA	N/A	N/A	7000.0	OEHHA
Toluene	N/A	N/A	5000.0	OEHHA	830.0	OEHHA	420.0	OEHHA
p-Benzoquinone	N/A	N/A	N/A	N/A	400.0	NIOSH	N/A	N/A

Note: URE values represent lifetime excess cancer risk per μg m^{-3}. REL and RfC values are in μg m^{-3} and represent non-cancer reference levels for short-term and chronic exposures, respectively. Abbreviations: OEHHA – Office of Environmental Health Hazard Assessment; EPA IRIS – Integrated Risk Information System; NIOSH – National Institute for Occupational Safety and Health. For grouping consistency, xylenes are used to represent C_8 aromatics, trimethylbenzenes for C_9 aromatics, and acrylic acid for methylglyoxal.

Table S2. Enhancement of individual VOCs during smoke-impacted periods

VOC	Mean (Smoke-impacted)	SD (Smoke-impacted)	Mean (Low-/no-smoke)	SD (Low-/no-smoke)	Enhancement factor
Methyl benzoic acid	0.015	0.013	0.002	0.002	7.809
Anisole	0.012	0.010	0.002	0.004	6.728
2-Furanone	0.055	0.044	0.010	0.007	5.549
5-Hydroxy-2-furfural / 2-furoic acid	0.059	0.045	0.011	0.007	5.428
Acrylonitrile*	0.030	0.025	0.006	0.005	5.279
Maleic anhydride*	0.104	0.101	0.020	0.020	5.094
Furfural	0.068	0.058	0.014	0.010	4.731
Methylfurfural	0.025	0.021	0.005	0.004	4.600
2-Furanmethanol	0.086	0.054	0.019	0.013	4.440
Methyl methacrylate*	0.152	0.090	0.037	0.026	4.156
2,3-Butanedione	0.354	0.201	0.088	0.055	4.020
Acrolein*	0.397	0.248	0.100	0.061	3.985
Acetic acid	3.928	2.152	1.027	0.628	3.825
MVK + MACR	0.365	0.194	0.097	0.075	3.748
Phenol*	0.033	0.025	0.009	0.006	3.711
p-Benzoquinone	0.041	0.028	0.011	0.006	3.700
2-Hydroxy-3-methyl-2-cyclopenten-1-one	0.046	0.027	0.013	0.009	3.650
Benzene*	0.680	0.451	0.202	0.152	3.358
Furan	0.047	0.048	0.014	0.014	3.305
Formic acid	3.029	1.703	0.919	0.511	3.295
Methylfuran	0.069	0.040	0.021	0.013	3.281
Benzofuran	0.008	0.006	0.002	0.002	3.255
Isocyanic acid	0.238	0.143	0.074	0.039	3.231
Cyclopentanone	0.067	0.034	0.021	0.013	3.181
2,5-Dimethylfuran	0.028	0.017	0.009	0.006	3.102
2-Pentanone	0.138	0.063	0.045	0.026	3.101

VOC	Mean (Smoke-impacted)	SD (Smoke-impacted)	Mean (Low-/no-smoke)	SD (Low-/no-smoke)	Enhancement factor
Nitromethane	0.128	0.066	0.042	0.022	3.085
Acetonitrile*	0.597	0.358	0.194	0.109	3.077
Acetaldehyde*	2.972	1.479	0.974	0.501	3.050
Guaiacol (2-methoxyphenol)	0.018	0.013	0.006	0.004	3.041
Naphthalene*	0.061	0.036	0.020	0.015	3.024
Dihydrofurandione	0.033	0.027	0.011	0.007	2.983
C3 Furans	0.026	0.014	0.009	0.007	2.882
PCBTF	0.022	0.032	0.008	0.006	2.837
Ethylcyclopentanone	0.014	0.007	0.005	0.003	2.801
MEK	0.404	0.227	0.146	0.139	2.765
Isoprene	0.769	0.445	0.283	0.245	2.718
Methanol*	16.256	6.793	6.156	3.382	2.641
Methylcyclopentanone / Cyclohexanone	0.038	0.019	0.014	0.009	2.631
1,2-Propanediol	0.110	0.046	0.043	0.021	2.554
Formaldehyde*	5.273	2.536	2.074	0.901	2.543
Methylglyoxal*	0.107	0.048	0.043	0.022	2.505
Formamide	0.122	0.055	0.049	0.023	2.501
Methanediol	0.074	0.045	0.030	0.022	2.500
Acetone	5.199	1.903	2.130	0.778	2.440
Toluene*	0.600	0.380	0.250	0.184	2.394
trans-2-Octenal	0.009	0.004	0.004	0.003	2.337
Hexanone	0.031	0.015	0.013	0.008	2.336
Cyclohexene	0.121	0.078	0.052	0.044	2.318
Propyne	1.500	0.757	0.653	0.379	2.298
Methyl isocyanate*	0.015	0.008	0.007	0.002	2.283
Methyl styrenes	0.026	0.016	0.012	0.009	2.211
C9 aromatics*	0.202	0.146	0.092	0.080	2.195

VOC	Mean (Smoke-impacted)	SD (Smoke-impacted)	Mean (Low-/no-smoke)	SD (Low-/no-smoke)	Enhancement factor
C8 aromatics*	0.574	0.392	0.272	0.244	2.114
1,3-Cyclopentadiene	0.065	0.026	0.031	0.018	2.072
Propene	0.633	0.362	0.310	0.193	2.041
Ethanol	6.278	3.832	3.111	2.090	2.018
Butenes	0.810	0.456	0.404	0.294	2.005
C10 aromatics	0.096	0.056	0.048	0.040	1.989
Nonene	0.004	0.002	0.002	0.001	1.945
Octanal	0.007	0.004	0.004	0.003	1.886
Texanol	0.004	0.002	0.002	0.001	1.872
Pentene / Methylbutenes	0.097	0.066	0.055	0.053	1.767
1,3-Butadiene*	0.518	0.313	0.293	0.197	1.766
D4 Siloxane	0.008	0.013	0.004	0.002	1.755
Benzaldehyde	0.070	0.042	0.040	0.036	1.722
Propiolic acid	0.004	0.003	0.003	0.001	1.706
Sesquiterpenes	0.008	0.004	0.005	0.004	1.627
D5 Siloxane	0.021	0.019	0.014	0.015	1.514
Dimethyl sulfide	0.024	0.011	0.016	0.009	1.488
Propanol	0.612	0.668	0.441	0.336	1.389
Dichlorobenzene*	0.012	0.005	0.008	0.003	1.388
Monoterpenes	0.644	0.432	0.514	0.506	1.253
Dimethyl trisulfide	0.030	0.024	0.029	0.024	1.028
Methanethiol	0.016	0.010	0.017	0.012	0.927
Ethylamine	0.003	0.001	0.003	0.001	0.887

Note: Smoke-impacted periods are defined as those with simultaneous enhancements in $PM_{2.5}$ ($\geq 12.5\ \mu g\ m^{-3}$), carbon monoxide (CO $\geq$ 150 ppb), and acetonitrile ($\geq$ 0.2 ppb). Enhancement factor is the ratio of the mean concentration during smoke-impacted periods to the mean concentration during low-/no-smoke periods. Mean and standard deviation (SD) are reported for each VOC under both conditions. All VOC concentrations are reported in parts per billion (ppb) by volume. Compounds marked with an asterisk (*) are listed as Hazardous Air Pollutants (HAPs) by the U.S. Environmental Protection Agency.

Table S3. Comparison of observed and literature enhancement ratios for individual VOCs.

Species	Integration EnR (This work)	RMA EnR (This work)	R^2 (This work)	Fiddler et al. 2024	Liu et al. 2017	Selimovic et al. 2018	Permar et al. 2021	Gkatzelis et al. 2024	Cope et al. 2024
Formaldehyde	11.41 ± 0.55	11.03 ± 1.05	0.500	8.310	23.790	17.550	18.220	17.920	24.500
Acetaldehyde	6.83 ± 0.32	6.45 ± 0.61	0.700	17.200	11.680	-	10.550	11.250	9.070
Acetone	8.90 ± 0.41	8.30 ± 0.79	0.600	5.450	6.100	-	4.061	4.040	8.790
Acetic acid	9.39 ± 0.48	9.92 ± 0.94	0.500	-	-	11.220	11.477	8.860	10.140
Formic acid	-	-	0.200	-	-	2.100	9.506	3.310	1.140
Methanol	29.74 ± 1.41	30.48 ± 2.87	0.600	-	18.960	12.920	13.165	10.900	29.710
Ethanol	-	-	0.100	-	-	-	-	-	-
1,2-Propanediol	0.22 ± 0.01	0.21 ± 0.02	0.500	-	-	-	-	-	-
2,3-Butanedione	0.91 ± 0.04	0.85 ± 0.08	0.600	-	-	-	-	-	-
2-Pentanone	0.31 ± 0.01	0.23 ± 0.02	0.700	-	-	-	-	-	-
Acetonitrile	1.52 ± 0.08	1.79 ± 0.17	0.800	2.310	1.910	-	2.090	2.040	0.790
Acrylonitrile	0.11 ± 0.00	0.14 ± 0.02	0.700	0.135	-	-	0.234	0.200	-
Isocyanic acid	0.55 ± 0.03	0.66 ± 0.07	0.500	-	-	-	-	-	-
Propyne	3.00 ± 0.15	3.22 ± 0.31	0.500	-	-	-	-	-	4.790
Propene	1.35 ± 0.07	1.63 ± 0.15	0.400	-	-	-	-	-	-
Butenes	-	-	0.300	-	-	-	-	-	-
Acrolein	1.13 ± 0.06	1.12 ± 0.11	0.800	1.800	-	-	1.872	3.730	-
Isoprene	-	-	0.100	-	-	-	-	-	-
Pentene / Methylbutenes	-	-	0	-	-	-	-	-	-
Cyclohexene	-	-	0.100	-	-	-	-	-	-
Methylfuran	-	-	0.300	-	-	-	0.918	0.400	0.070
Furfural	0.21 ± 0.01	0.28 ± 0.03	0.400	-	-	3.060	1.519	0.520	-

Species	Integration EnR (This work)	RMA EnR (This work)	R^2 (This work)	Fiddler et al. 2024	Liu et al. 2017	Selimovic et al. 2018	Permar et al. 2021	Gkatzelis et al. 2024	Cope et al. 2024
2-Furanmethanol	0.23 ± 0.01	0.21 ± 0.02	0.500	-	-	-	-	-	-
2-Furanone	0.17 ± 0.01	0.21 ± 0.02	0.400	-	-	-	-	-	-
Benzene	2.02 ± 0.10	2.19 ± 0.20	1	2.770	1.730	-	1.764	2.260	1.290
Toluene	1.30 ± 0.07	1.75 ± 0.17	0.600	3.300	0.820	-	1.230	1.420	2.070
C8 aromatics	1.32 ± 0.08	1.84 ± 0.18	0.400	0.660	0.440	-	0.530	-	3
C9 aromatics	0.48 ± 0.03	0.71 ± 0.07	0.400	-	-	-	0.156	0.130	0.710
C10 aromatics	-	-	0.300	-	-	-	0.081	-	0.210
Naphthalene	0.15 ± 0.01	0.18 ± 0.02	0.400	-	-	-	-	-	-
Methylglyoxal	-	-	0.100	-	-	-	-	-	-
Cyclopentanone	0.15 ± 0.00	0.14 ± 0.02	0.500	-	-	-	-	-	-
Methyl methacrylate	0.38 ± 0.02	0.32 ± 0.03	0.600	-	-	-	0.315	-	-
MEK	0.94 ± 0.05	1.01 ± 0.10	0.800	1.110	-	-	0.816	0.840	2.640
MVK + MACR	-	-	0.300	1.160	1.480	-	1.559	2.560	0.500
Nitromethane	0.32 ± 0.01	0.29 ± 0.03	0.700	-	-	-	0.376	0.230	-
Formamide	0.23 ± 0.01	0.21 ± 0.02	0.500	-	-	-	-	-	-
Monoterpenes	-	-	0	-	-	-	-	-	-

Note: Enhancement ratios (EnRs) are expressed relative to CO (ppb ppm^{-1}). Values represent observed integration-based and reduced-major-axis (RMA) estimates along with literature ranges for fresh and aged smoke plumes (Cope et al., 2024; Fiddler et al., 2024; Gkatzelis et al., 2024; Liu et al., 2017; Permar et al., 2021; Selimovic et al., 2018). Dashes denote unavailable data.

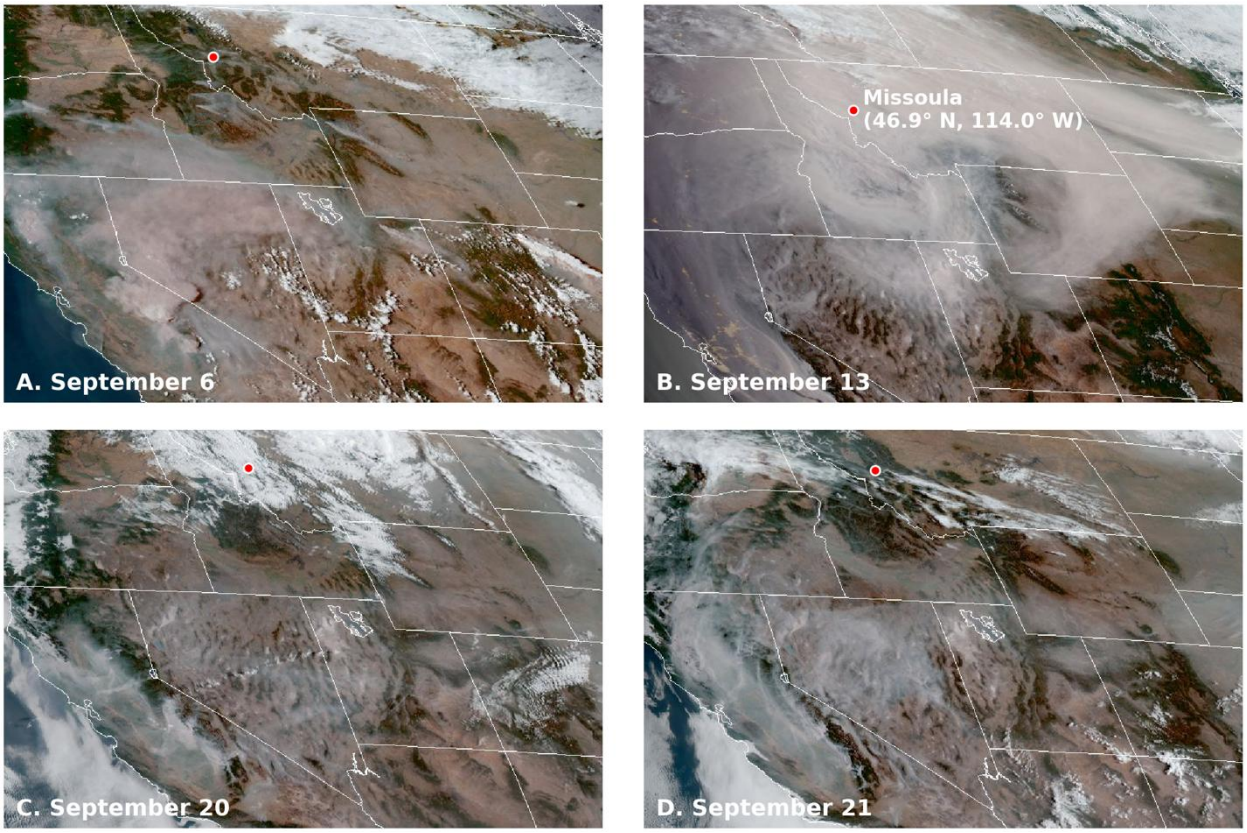

Figure S1. Western U.S. wildfire smoke extent during four representative days in September 2020, captured by GOES GeoColor imagery. Panels show true-color satellite images from the GOES-17 Advanced Baseline Imager (ABI) on (A) September 6 (5:40 PM), (B) September 13 (8:50 AM), (C) September 20 (9:30 AM), and (D) September 21 (9:20 AM), highlighting regional smoke coverage and plume evolution across the western United States. The red dot marks Missoula, Montana (46.9° N, 114.0° W), the site of ground-based air quality measurements discussed in the main text. Each image is cropped to a consistent spatial domain (approximately 36°–50.8° N latitude, 101°–122° W longitude).

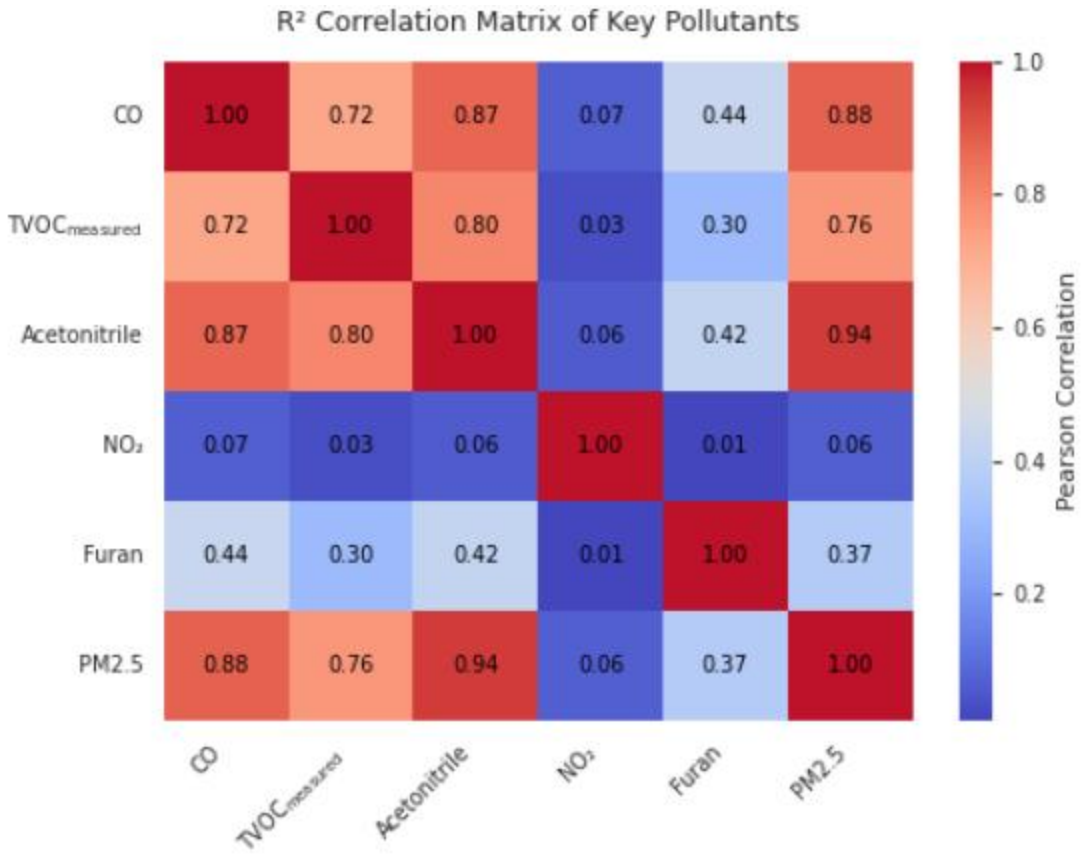

Figure S2. Relationship among key air pollutants during wildfire smoke influence in Missoula, Montana. Shown are coefficients of determination (R^2) between hourly measurements of $PM_{2.5}$, carbon monoxide (CO), total volatile organic compounds (VOCs), acetonitrile, nitrogen dioxide (NO_2), and furan. All variables are reported in parts per billion (ppb), except $PM_{2.5}$ in micrograms per cubic meter ($\mu g\ m^{-3}$). Correlations are based on data collected at hourly resolution during September 2020.

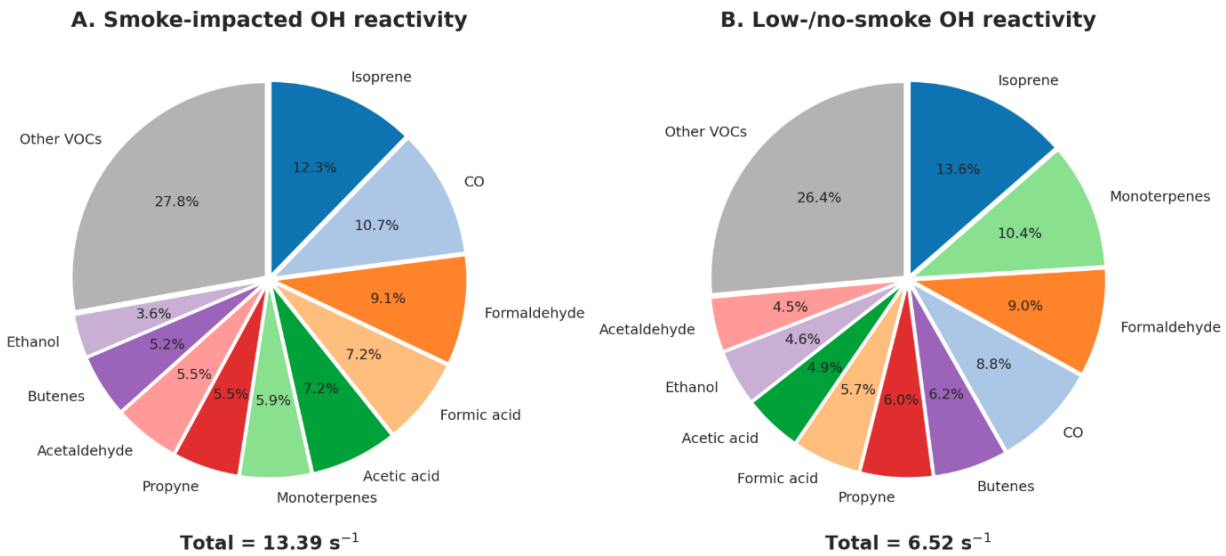

Figure S3. Fractional contributions of CO and measured VOCs to OH reactivity in Missoula in September 2020. (A) Composition of total measured OH reactivity (s^{-1}) during smoke-impacted periods. (B) Composition of OH reactivity during low- or no-smoke periods. Slices show mean hourly fractional OHR of the largest contributors; all other minor contributors (< 2 % each) are aggregated as “Other VOCs”.

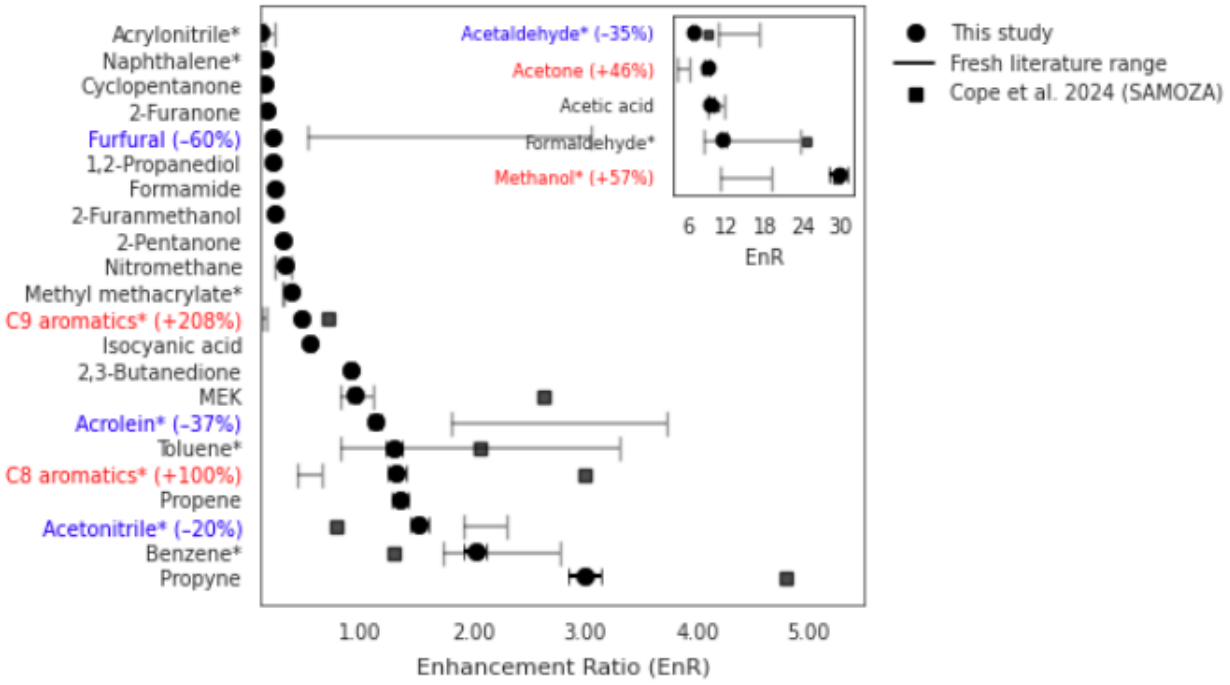

Figure S4. Event-integrated enhancement ratios (EnR) of volatile organic compounds (VOCs) relative to CO in biomass-burning plumes. Black circles with error bars show EnRs from this study (mean ± 1σ), ordered by decreasing magnitude. Compounds labeled with an asterisk (*) are U.S. EPA hazardous air pollutants. Values reported in this study exceeding EnR = 5 are displayed on a compressed inset axis to preserve the main scale. The gray error bars indicate the range of fresh-smoke EnRs reported in previous studies (Fiddler et al., 2024; Liu et al., 2017; Permar et al., 2021; Gkatzelis et al., 2024; Selimovic et al., 2018). Black squares show aged-smoke values observed downwind (Cope et al., 2024). Species labels are highlighted when EnRs from this study fall outside the reported fresh-smoke range after accounting for calibration and uncertainty constraints. The numerical values of individual VOC EnRs are provided in Table S3.

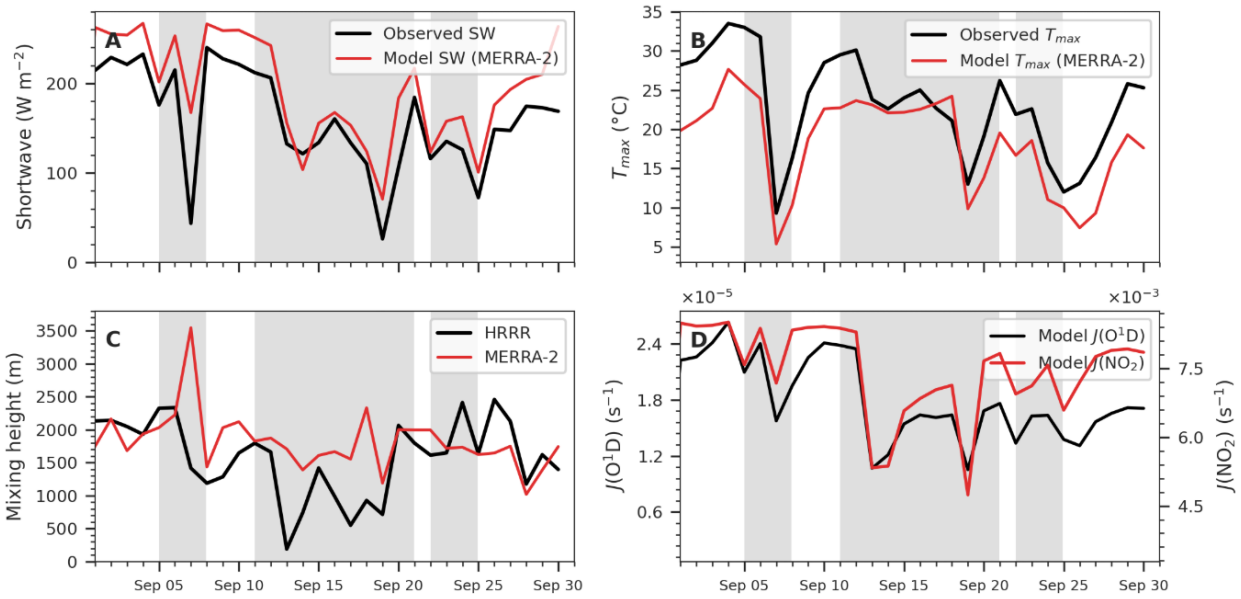

Figure S5. Meteorological and photolysis diagnostics during September 2020 in Missoula, Montana. (A) Daily mean downwelling shortwave radiation from surface observations (black) and the MERRA-2 meteorological reanalysis used to drive GEOS-Chem (red). (B) Daily maximum near-surface air temperature from observations (black) and MERRA-2 (red). (C) Daily maximum planetary boundary layer height (PBLH) from HRRR (black) and MERRA-2 (red). (D) Daily maximum photolysis frequencies from GEOS-Chem: $J(O^1D)$ (left axis, black) and $J(NO_2)$ (right axis, red). In all panels, gray shading denotes periods classified as smoke-impacted based on surface observations.

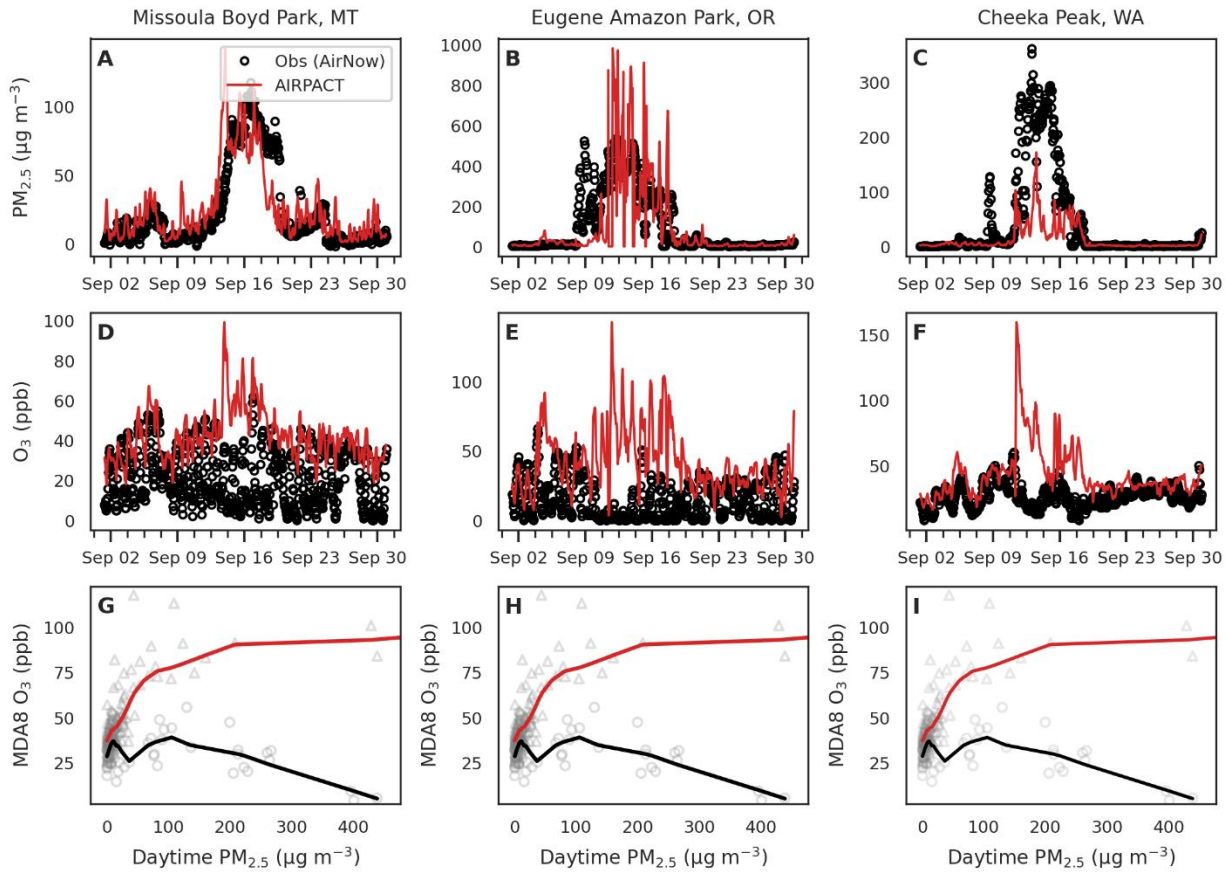

Figure S6. Observed and AIRPACT-simulated $PM_{2.5}$ and ozone time series and their joint behavior during September 2020 at three western U.S. sites. Hourly $PM_{2.5}$ time series from surface observations (open black circles) and the AIRPACT forecast system (solid red lines) at (A) Missoula Boyd Park, MT; (B) Eugene Amazon Park, OR; and (C) Cheeka Peak, WA. Panels (D–F) show the corresponding hourly O_3 time series at the same sites and in the same order. Panels (G–I) show the relationship between daily maximum 8-hour average ozone (MDA8 O_3, ppb) and daytime mean $PM_{2.5}$ (µg m^{-3}) for each site, derived from surface observations and AIRPACT simulations. Daytime $PM_{2.5}$ is calculated as the 10:00–20:00 local-time average. Solid curves indicate locally weighted scatterplot smoothing (LOWESS; span = 0.5). AIRPACT outputs are sampled in space and time at the monitoring locations and were obtained from the Washington State University AIRPACT data portal (https://airpact.wsu.edu/).

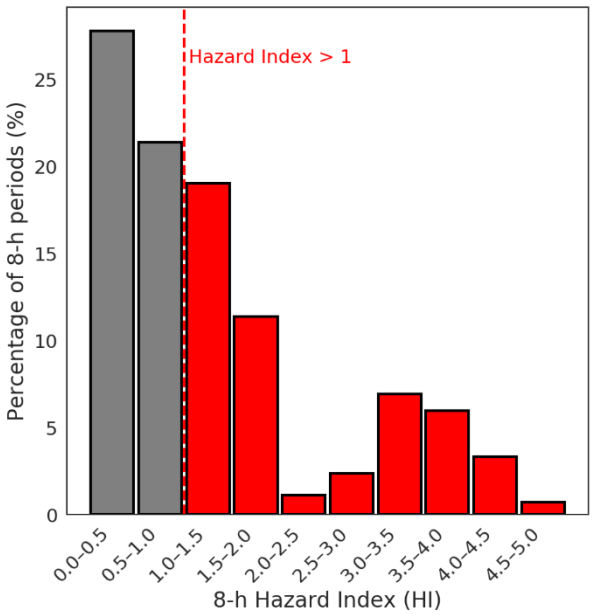

Figure S7. Distribution of 8-h hazard index (HI) values for gaseous pollutants during smoke-impacted periods. The histogram bins (0.5-unit width) show the fraction of all 8-h intervals falling into each HI range, expressed as a percentage of all 8-h intervals. Gray bars correspond to HI ≤ 1 (no expected adverse health effect), while red bars indicate HI > 1 (potential health risk). The dashed vertical line at HI = 1 and its annotation mark the threshold above which cumulative exposures may pose noncancer health concerns.

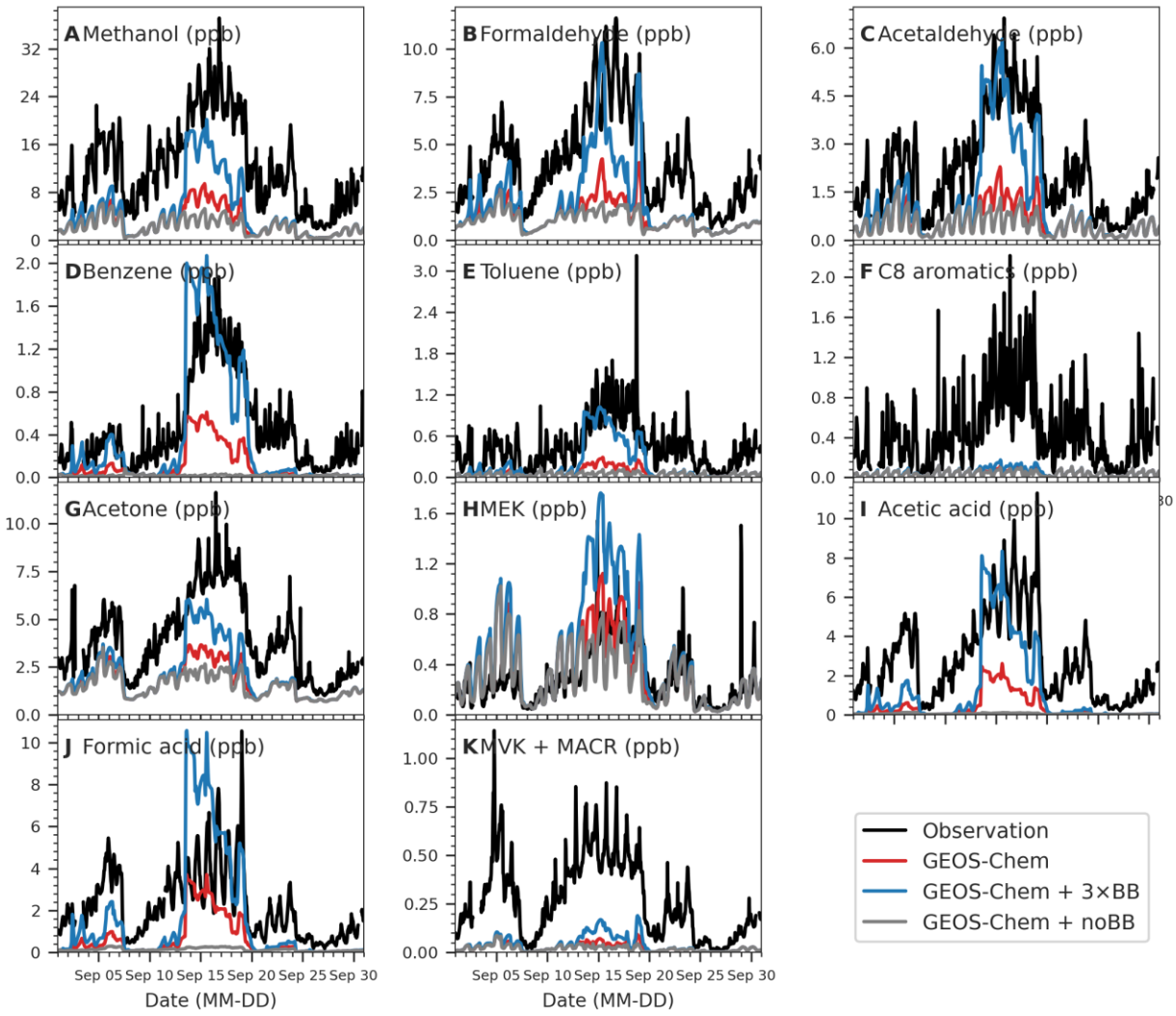

Figure S8. Time series of observed and modeled concentrations for VOCs during September 2020 in Missoula, MT. Observations (black lines) are compared with GEOS-Chem driven by GFAS v1.2 biomass burning emission inventory (red). Also shown are two model sensitivity tests with biomass-burning emissions turned off (GEOS-Chem + noBB; gray) and with tripled GFAS v1.2 emissions (GEOS-Chem + 3×BB; blue). Model outputs are sampled at the observational location and time. Gray shading indicates periods classified as smoke-impacted.

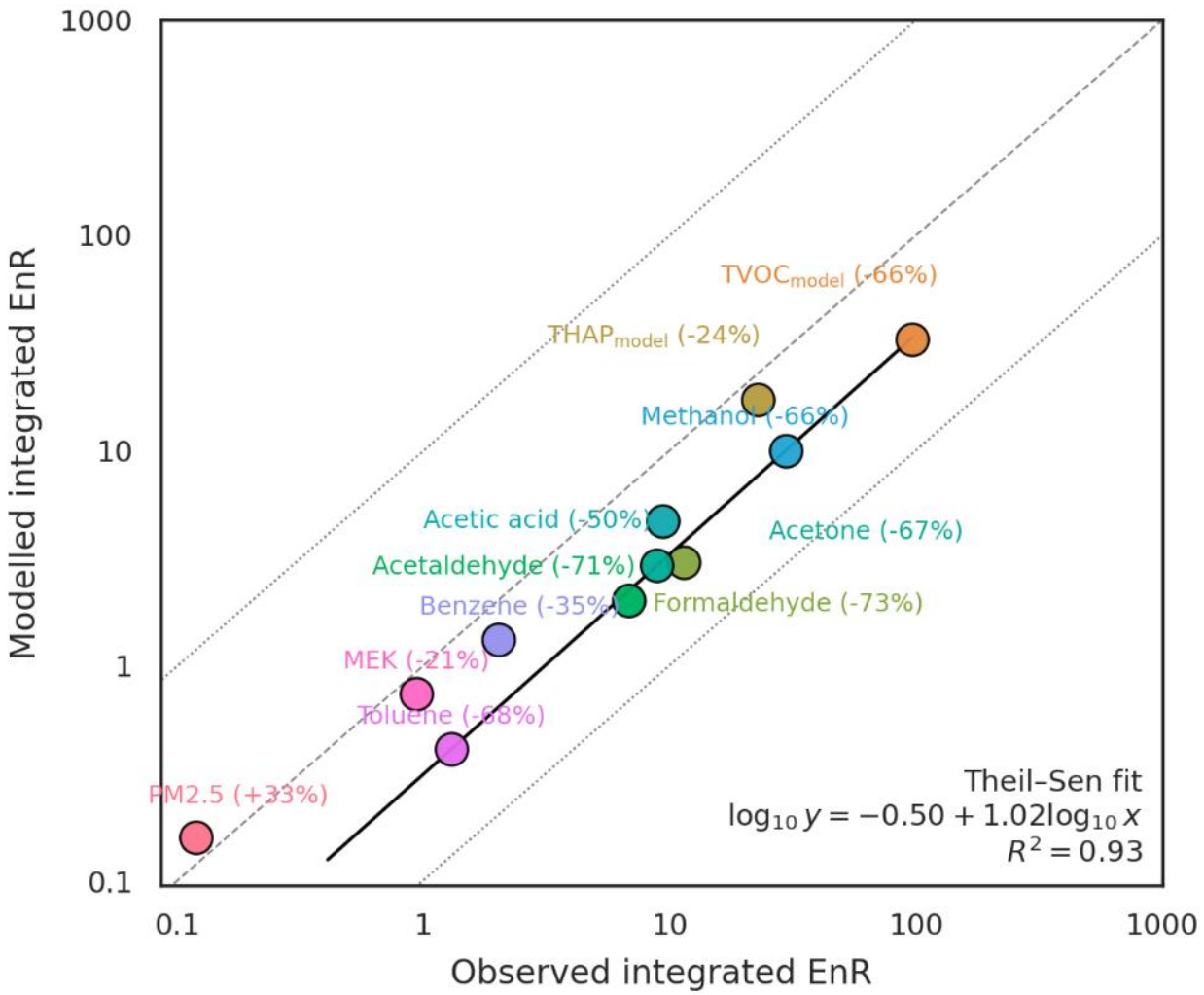

Figure S9. Event-integrated enhancement ratios (EnRs) relative to CO from observations and the GEOS-Chem simulation for smoke, shown on logarithmic axes. Data are integrated EnRs for smoke Event 2, colored by individual species with their species names and model relative biases labeled. VOC EnRs are expressed in ppb ppm^{-1} CO, while the $PM_{2.5}$ EnR is in g g^{-1}. The black solid line shows the Theil–Sen log–log regression (equation and R^2 given in the inset). The gray dashed line indicates 1:1 agreement and dotted lines indicate ±1 order of magnitude. Points below (above) the 1:1 line indicate under- (over-) prediction of integrated EnR in the model.

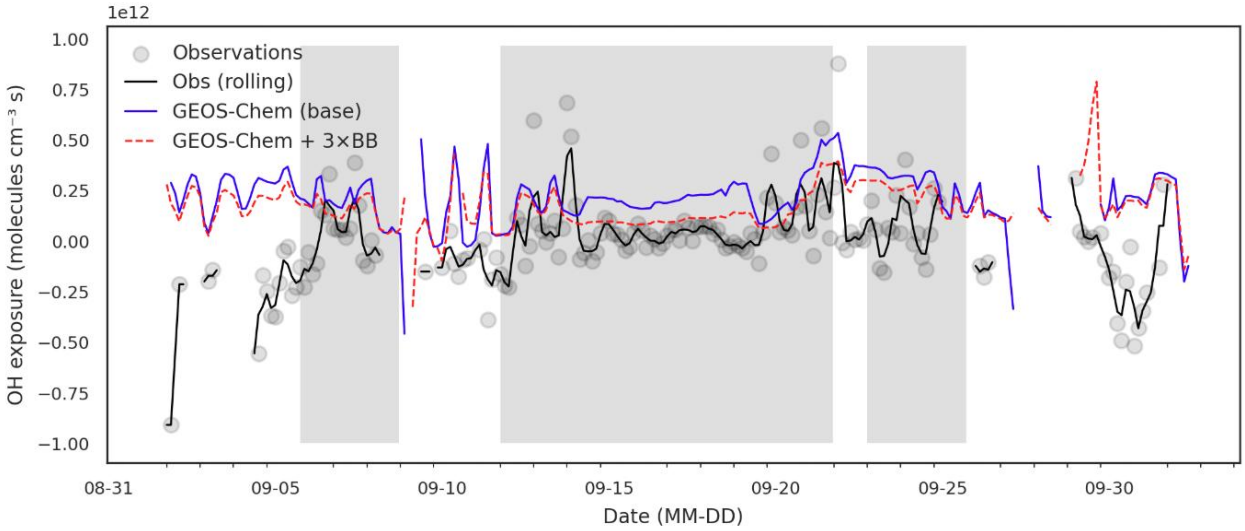

Figure S10. **Time series comparison of observed and modeled OH exposure for the September smoke period**. Observations (gray circles; 3-hour medians) and their 3-point centered rolling mean (black line) are plotted against GEOS-Chem simulations driven by the Global Fire Assimilation System (blue) and a sensitivity run with 3×BB emissions (red dashed). Gray bands denote hours classified as smoke-impacted. All series are binned every three hours. Major x-axis ticks occur every 5 days with minor daily ticks. OH exposure (molecules cm^{-3} s) is inferred from a photochemical clock based on toluene-to-benzene ratios.

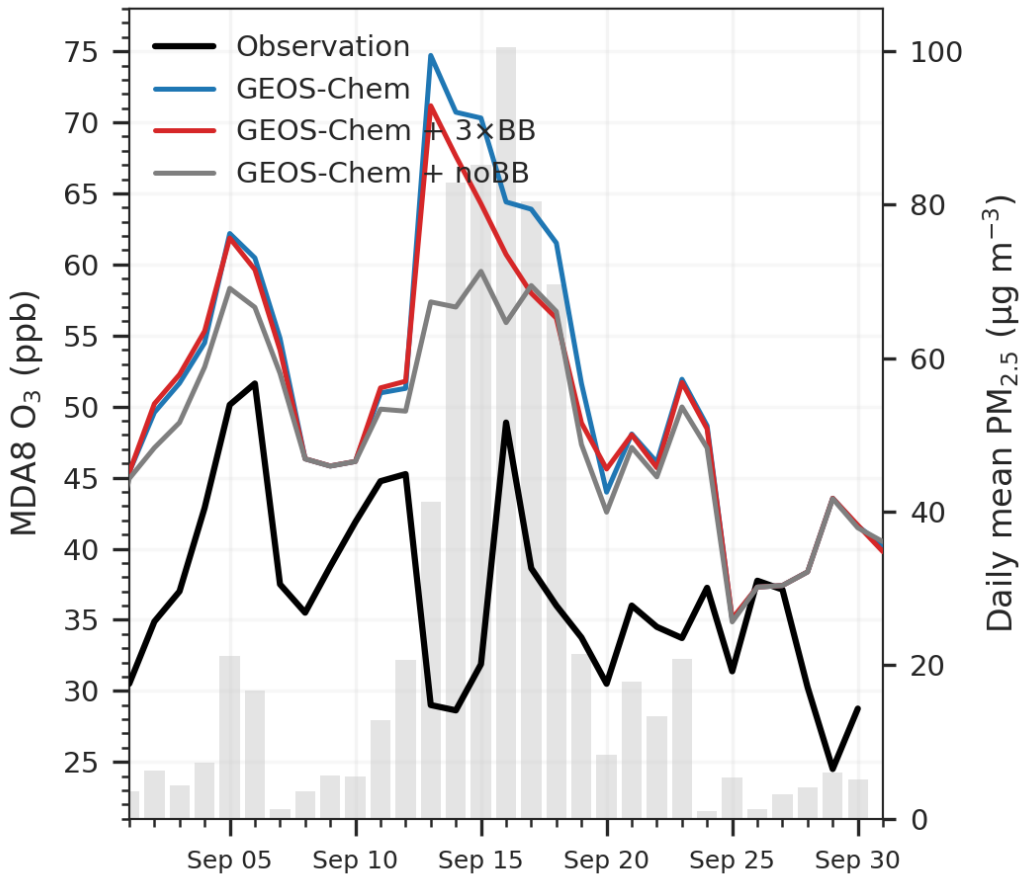

Figure S11. **Temporal evolution of daily maximum 8-hour ozone during September and its relationship to smoke influence**. Time series of daily maximum 8-hour average ozone (MDA8 O_3, ppb) from surface observations (black) and GEOS-Chem simulations driven by standard GFAS fire emissions (blue), enhanced fire emissions (GEOS-Chem + 3×BB; red), and a no-biomass-burning configuration (GEOS-Chem + noBB; gray). Shaded bars (right axis) indicate observed daytime $PM_{2.5}$ (µg m^{-3}), which is calculated as the 10:00–20:00 local-time mean.

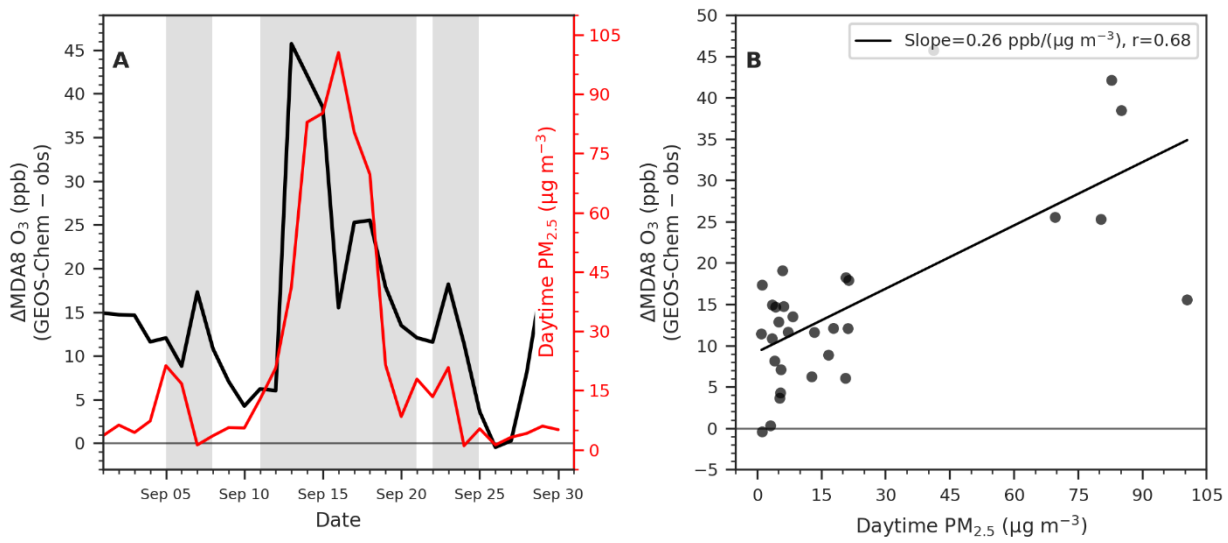

Figure S12. Relationship between ozone model bias and particulate matter during wildfire smoke events in Missoula, Montana. (A) Daily ozone bias (ΔMDA8 O_3 = GEOS-Chem − observation; ppb, black; left axis) during September 2020 compared with observed daytime $PM_{2.5}$ concentrations (μg m^{-3}; red; right axis). Gray shading denotes smoke-impacted periods identified from local air-quality observations. (B) Dependence of daily ozone bias (ΔMDA8 O_3) on daytime $PM_{2.5}$. Each point represents a daily average. The solid line shows an ordinary least-squares (OLS) linear regression fitted to the data, with the reported correlation coefficient. Daytime $PM_{2.5}$ is calculated as the 10:00–20:00 local-time mean.

References

Centers for Disease Control and Prevention (CDC): NIOSH Pocket Guide to Chemical Hazards, National Institute for Occupational Safety and Health, https://www.cdc.gov/niosh/npg/default.html (last access: 30 July 2026), 2020.

Cope, E. M., Ketcherside, D. T., Jin, L., Tan, L., Mansfield, M., Jones, C., Lyman, S., Jaffe, D., and Hu, L.: Sources of Atmospheric Volatile Organic Compounds During the Salt Lake Regional Smoke, Ozone and Aerosol Study (SAMOZA) 2022, J. Geophys. Res.-Atmos., 129, e2024JD041640, https://doi.org/10.1029/2024JD041640, 2024.

de Gouw, J. A., Gilman, J. B., Kim, S. W., Lerner, B. M., Isaacman-VanWertz, G., McDonald, B. C., Warneke, C., Kuster, W. C., Lefer, B. L., Griffith, S. M., Dusanter, S., Stevens, P. S., and Stutz, J.: Chemistry of Volatile Organic Compounds in the Los Angeles basin: Nighttime Removal of Alkenes and Determination of Emission Ratios, J. Geophys. Res.-Atmos., 122, 11843–11861, https://doi.org/10.1002/2017JD027459, 2017.

Fiddler, M. N., Thompson, C., Pokhrel, R. P., Majluf, F., Canagaratna, M., Fortner, E. C., Daube, C., Roscioli, J. R., Yacovitch, T. I., Herndon, S. C., and Bililign, S.: Emission Factors From Wildfires in the Western US: An Investigation of Burning State, Ground Versus Air, and Diurnal Dependencies During the FIREX-AQ 2019 Campaign, J. Geophys. Res.-Atmos., 129, e2022JD038460, https://doi.org/10.1029/2022JD038460, 2024.

Gkatzelis, G. I., Coggon, M. M., Stockwell, C. E., Hornbrook, R. S., Allen, H., Apel, E. C., Bela, M. M., Blake, D. R., Bourgeois, I., Brown, S. S., Campuzano-Jost, P., St. Clair, J. M., Crawford, J. H., Crounse, J. D., Day, D. A., DiGangi, J. P., Diskin, G. S., Fried, A., Gilman, J. B., Guo, H., Hair, J. W., Halliday, H. S., Hanisco, T. F., Hannun, R., Hills, A., Huey, L. G., Jimenez, J. L., Katich, J. M., Lamplugh, A., Lee, Y. R., Liao, J., Lindaas, J., McKeen, S. A., Mikoviny, T., Nault, B. A., Neuman, J. A., Nowak, J. B., Pagonis, D., Peischl, J., Perring, A. E., Piel, F., Rickly, P. S., Robinson, M. A., Rollins, A. W., Ryerson, T. B., Schueneman, M. K., Schwantes, R. H., Schwarz, J. P., Sekimoto, K., Selimovic, V., Shingler, T., Tanner, D. J., Tomsche, L., Vasquez, K. T., Veres, P. R., Washenfelder, R., Weibring, P., Wennberg, P. O., Wisthaler, A., Wolfe, G. M., Womack, C. C., Xu, L., Ball, K., Yokelson, R. J., and Warneke, C.: Parameterizations of US wildfire and prescribed fire emission ratios and emission factors based on FIREX-AQ aircraft measurements, Atmos. Chem. Phys., 24, 929–956, https://doi.org/10.5194/acp-24-929-2024, 2024.

Koss, A. R., Sekimoto, K., Gilman, J. B., Selimovic, V., Coggon, M. M., Zarzana, K. J., Yuan, B., Lerner, B. M., Brown, S. S., Jimenez, J. L., Krechmer, J., Roberts, J. M., Warneke, C., Yokelson, R. J., and de Gouw, J.: Non-methane organic gas emissions from biomass burning: identification, quantification, and emission factors from PTR-ToF during the FIREX 2016 laboratory experiment, Atmos. Chem. Phys., 18, 3299–3319, https://doi.org/10.5194/acp-18-3299-2018, 2018.

Liu, X., Huey, L. G., Yokelson, R. J., Selimovic, V., Simpson, I. J., Müller, M., Jimenez, J. L., Campuzano-Jost, P., Beyersdorf, A. J., Blake, D. R., Butterfield, Z., Choi, Y., Crounse, J. D., Day, D. A., Diskin, G. S., Dubey, M. K., Fortner, E., Hanisco, T. F., Hu, W., King, L. E., Kleinman, L., Meinardi, S., Mikoviny, T., Onasch, T. B., Palm, B. B., Peischl, J., Pollack, I. B., Ryerson, T. B., Sachse, G. W., Sedlacek, A. J., Shilling, J. E., Springston, S., St. Clair, J. M., Tanner, D. J., Teng, A. P., Wennberg, P. O., Wisthaler, A., and Wolfe, G. M.: Airborne measurements of western U.S. wildfire emissions: comparison with prescribed burning and air quality implications, J. Geophys. Res.-Atmos., 122, 6108–6129, https://doi.org/10.1002/2016JD026315, 2017.

Office of Environmental Health Hazard Assessment (OEHHA): OEHHA acute, 8-hour and chronic Reference Exposure Level (REL) summary, https://oehha.ca.gov/air/general-info/oehha-acute-8-hour-and-chronic-reference-exposure-level-rel-summary (last access: 30 July 2026), 2023.

Office of Environmental Health Hazard Assessment (OEHHA): Appendix A: Hot Spots Unit Risk and Cancer Potency Values, updated January 2025, https://oehha.ca.gov/media/downloads/crnr/appendixa.pdf (last access: 30 July 2026), 2025.

Permar, W., Wang, Q., Selimovic, V., Wielgasz, C., Yokelson, R. J., Hornbrook, R. S., Hills, A. J., Apel, E. C., Ku, I., Zhou, Y., Sive, B. C., Sullivan, A. P., Collett, J. L., Campos, T. L., Palm, B. B., Peng, Q., Thornton, J. A., Garofalo, L. A., Farmer, D. K., Kreidenweis, S. M., Levin, E. J. T., DeMott, P. J., Flocke, F., Fischer, E. V., and Hu, L.: Emissions of trace organic gases from western U.S. wildfires based on WE-CAN aircraft measurements, J. Geophys. Res.-Atmos., 126, e2020JD033838, https://doi.org/10.1029/2020JD033838, 2021.

Pye, H. O. T., Xu, L., Henderson, B. H., Pagonis, D., Campuzano-Jost, P., Guo, H., Jimenez, J. L., Allen, C., Skipper, T. N., Halliday, H. S., Murphy, B. N., D'Ambro, E. L., Wennberg, P. O., Place, B. K., Wiser, F. C., McNeill, V. F., Apel, E. C., Blake, D. R., Coggon, M. M., Crounse, J. D., Gilman, J. B., Gkatzelis, G. I., Hanisco, T. F., Huey, L. G., Katich, J. M., Lamplugh, A., Lindaas, J., Peischl, J., St. Clair, J. M., Warneke, C., Wolfe, G. M., and Womack, C.: Evolution of Reactive Organic Compounds and Their Potential Health Risk in Wildfire Smoke, Environ. Sci. Technol., 58, 19785–19796, https://doi.org/10.1021/acs.est.4c06187, 2024.

Selimovic, V., Yokelson, R. J., Warneke, C., Roberts, J. M., de Gouw, J., Reardon, J., and Griffith, D. W. T.: Aerosol optical properties and trace gas emissions by PAX and OP-FTIR for laboratory-simulated western US wildfires during FIREX, Atmos. Chem. Phys., 18, 2929–2948, https://doi.org/10.5194/acp-18-2929-2018, 2018.

U.S. Environmental Protection Agency (US EPA): Technical Support Document: EPA's Air Toxics Screening Assessment – 2018 AirToxScreen TSD, EPA-452/B-22-002, Office of Air Quality Planning and Standards, Research Triangle Park, NC, https://www.epa.gov/AirToxScreen/airtoxscreen-technical-support-document (last access: 30 July 2026), 2022.

U.S. Environmental Protection Agency (US EPA): IRIS Toxicological Review of Formaldehyde (Inhalation) (Final Report, 2024), EPA/635/R-24/162, Integrated Risk Information System, Office of Research and Development, Washington, DC, https://iris.epa.gov/static/pdfs/0419tr.pdf, 2024.

U.S. Environmental Protection Agency (US EPA): Integrated Risk Information System (IRIS), https://www.epa.gov/iris (last access: 30 July 2026), 2026.